Transp Porous Med (2008) 74:35–47
DOI 10.1007/s11242-007-9179-3

Wetting Phase Bridges Establish Capillary Continuity Across Open Fractures and Increase Oil Recovery in Mixed-Wet Fractured Chalk

Eirik Aspenes · Geir Ersland · Arne Graue · Jim Stevens · Bernard A. Baldwin

Received: 26 November 2006 / Accepted: 19 October 2007 / Published online: 6 November 2007

Abstract The effect of fractures on oil recovery and in situ saturation development in fractured chalk has been determined at near neutral wettability conditions. Fluid saturation development was monitored both in the matrix and in the fractures and the mechanisms of fracture crossing were determined using high spatial resolution MRI. Capillary continuity across open oil-filled fractures was verified by imaging the water bridges established within the fracture. Despite an alternate escape fracture for the water, separate water bridges were shown to be stable for the entire duration of the experiments. The established capillary contact resulted in oil recovery exceeding the spontaneous imbibition potential in the outlet-isolated cores by ca. 10% PV. This is explained by viscous recovery provided by water bridges across open fractures. The size of the bridges seemed to be controlled by the wettability of the rock and not by the differential pressure applied across the open fracture.

Keywords Capillary continuity · Fractures · IOR · MRI · Chalk · Wettability

1 Introduction

In fractured chalk reservoirs, it has generally been believed that oil production results from spontaneous imbibition of water into individual matrix blocks from the fracture network followed by a subsequent displacement of the expelled oil through the fractures toward the

E. Aspenes · G. Ersland · A. Graue (✉)
Department of Physics and Technology, University of Bergen, Allegaten 55, Bergen 5007, Norway
e-mail: arne.graue@ift.uib.no

J. Stevens
ConocoPhillips, Bartlesville, USA

B. A. Baldwin
Green Country Petrophysics LLC, Dewey, OK, USA

Present Address:
E. Aspenes
Statoil ASA, Stavanger, Norway

production wells. However, several authors, (Thomas et al. 1987; Sulak 1990; Hermansen et al. 1998; Agarwal et al. 1999) suggest that if there were a significant amount of capillary continuity between adjacent blocks, viscous displacement of oil could also play a role and the matrix pore network could provide an alternate path for oil movement toward the producing wells. Capillary continuity would preserve the hydraulic continuum in the water phase over fractures and transfer the injection pressure needed for viscous oil recovery. Viscous displacement due to the presence of a pressure gradient during waterfloods would have the best potentials in reservoirs which are less than strongly water-wet (Hermansen et al. 2000).

Several authors have reported laboratory experiments investigating capillary communication between matrix blocks (Saidi et al. 1979; Horie et al. 1990; Firozabadi and Hauge 1990; Labastie 1990; Stones et al. 1992). However, these experiments were conducted in vertically stacked porous media with the objective of obtaining a better understanding of gas/oil gravity drainage.

Fluid flow across fractures between adjacent matrix blocks in chalk has been studied since the early 1990s (Graue et al. 1990, 1999b). Experiments with larger scale fractured block systems and smaller scale stacked core plugs determined production mechanisms and their dependency on reservoir parameters such as wettability, differential pressure, fracture aperture, and fracture configuration.

The oil recovery mechanisms involved while waterflooding fractured chalk blocks were found to be dependent on the wettability of the chalk (Viksund et al. 1996, 1997; Graue et al. 1999a, 2000a, b, 2001a, b, 2002a, b, 2003; Aspenes et al. 2002a). At strongly water-wet conditions, water accumulated in the preceding matrix block until the spontaneous imbibition endpoint was reached. Then water entered the fracture and moved into the next matrix block expelling the oil on a block-by-block basis. At moderately water-wet conditions, however, water moved across the fractures at lower water saturations, propagating through the system as in a continuous block. This was attributed to the establishment of capillary continuity between the matrix blocks by establishing wetting phase bridges and thus adding a viscous recovery component to the oil displacement. The obtained capillary continuity is schematically illustrated in Fig. 1, where wetting phase bridges preserve the hydraulic continuum in the water phase over open oil-filled fractures. Two complimentary imaging techniques were used to monitor water movement. Nuclear Tracer Imaging (NTI), (Bailey 1981) provided macroscopic information of the dynamics of the water saturation in large blocks of chalk with a spatial resolution of ca. 1 cm. The NTI technique is described in Lien et al. (1988), Graue et al. (1990), Graue (1994). Magnetic Resonance Imaging (MRI) was utilized to visualize fluid flow inside the open fracture between two core plugs (Graue et al. 2001b). The spatial resolution of the MRI images is on the order of 100 μm. In addition, water floods carried out on the large block samples were history-matched using a full field numerical simulator. Both the production data and in situ saturation development during the water floods were matched at the different wettability conditions (Graue et al. 2000a).

In the previous MRI experiments, flow across fractures, using stacked core plugs separated by an open fracture was investigated. The core system was sleeved and the wetting phase was thus forced to cross the fracture into the next core. In order to expand the understanding of the recovery mechanisms, during waterfloods in fractured low permeable rock, a fracture network with an alternate flow path, an escape fracture, was created. The experiments presented in this work contain an open vertical slit from the transverse fracture to the outlet (Fig. 2). This slit provides a path for the wetting phase to escape the system without going into the isolated matrices. However, if stable wetting phase bridges, observed in earlier stacked core experiments, form across open fractures, a viscous force applied to the isolated matrices would increase recovery beyond the spontaneous imbibition potential.

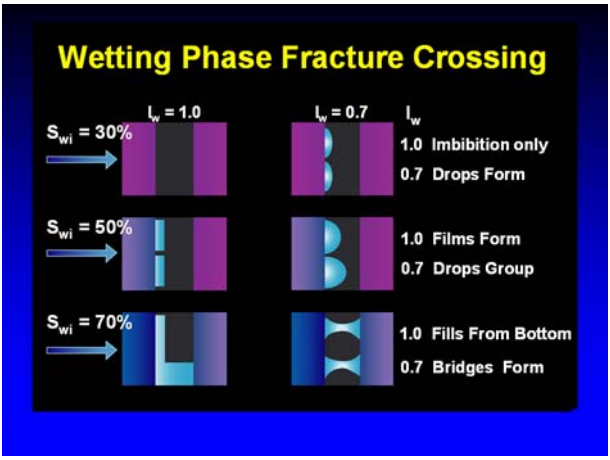

Fig. 1 Schematic of capillary continuity across fractures for various wettabilities. The capillary attraction to water from the fracture surfaces allow stable bridging over open oil-filled fractures (Aspenes et al. 2002)

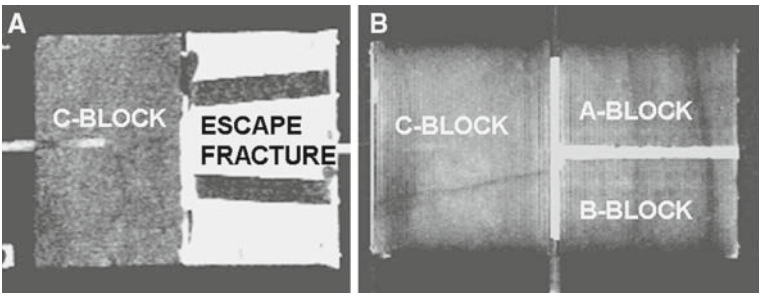

Fig. 2 (**a**) MRI image showing the vertical central slice through the C-Block and the vertical escape fracture (side-view). (**b**) MRI image showing a horizontal slice through the stacked core system (top-view)

2 Experimental

2.1 Core Preparation and Wettability Conditions

The core plug used was a 3.8 cm diameter, 5.7 cm long chalk core plug. The core plug was drilled from quarried pieces of Rørdal outcrop chalk obtained from the Portland quarry at Ålborg, Denmark. Description of this material can be found in Lie (1995). The core plug was dried at 60°C for 3 days, vacuum evacuated to 10 mBar and saturated with degassed brine containing 5.0 wt% NaCl, 3.8 wt% $CaCl_2$ (5 wt% $CaCl_2 \cdot 2H_2O$), and 0.01 wt% NaN_3. Weight measurements before and after vacuum saturation, gave an estimated pore volume of 30.7 ml and porosity of 47.1%. Absolute brine permeability was measured to be 3.5 mD.

It has been shown that upon controlled exposure to crude oil, the surface of strongly water-wet outcrop chalk may be rendered less water-wet (Graue et al. 1999b). A stock tank crude oil from a North Sea chalk reservoir was used to alter the wettability of the core plug. Initial water saturation, $S_{wi} = 28\%$ PV, was established by oil flooding with a maximum differential pressure of 2 bar/cm. Wettability alteration of the core plug was achieved by continuously flushing the stock tank crude oil through the core at 80°C with a Darcy velocity of 0.4 cm/h

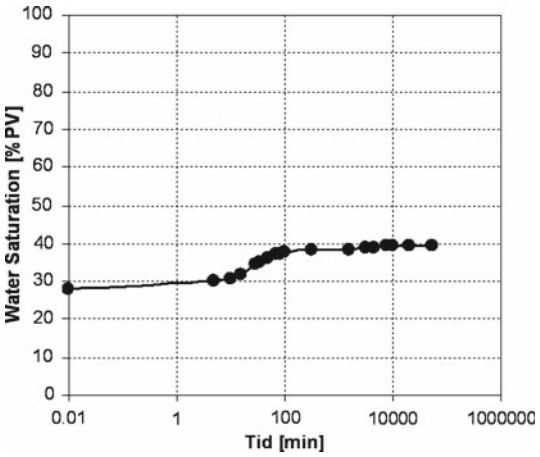

Fig. 3 Whole core spontaneous imbibition curve

for 24 h; with flow direction altered mid-way between the conditioning. The crude oil was filtered through a 3 cm long, 3.8 cm diameter Rørdal chalk core plug at 80°C before the sample was oil flooded. A backpressure of four bars minimized gas flash from the heated oil. The aging-while-flushing procedure is more efficient and generates uniform wettability distributions compared to conventional static aging techniques; where the core sample is submerged in crude oil. The aging procedure was previously published in Aspenes et al. (2002b) and Graue et al.(2002a).

After aging, the crude oil was subsequently exchanged with five pore volumes of decahydronapthalene (decalin) and five pore volumes of *n*-decane, at 80°C. When the core cooled to room temperature, it was subjected to spontaneous imbibition by submersion in brine. The spontaneous imbibition production versus time is shown in Fig. 3. The induction time, i.e., the time before imbibition starts, is 10 min, and significantly longer compared to a strongly water-wet plug, indicating weaker capillary forces, alternatively indicating the presence of an oil film on the outside surface of the aged core plug or reflecting the time needed to establish counter current flow conditions with respect to relative permeabilities. The endpoint for imbibition at 39% water saturation was reached after 39 days. This yields an oil recovery of 15% OIP. After the forced water flood, the water saturation was 58% PV, yielding an Amott index to water of 0.3 (Amott 1959). The stability of the wettability alteration for this chalk by crude oil adsorption has earlier been proven excellent (Aspenes et al. 2002b).

2.2 Preparation for Fracture Crossing Experiments

The desired fracture network was created using a band saw. To ensure a continuous wettability distribution across the fractures, the fracture network was created within a single core plug. Thus, the core plug was cut into two plugs, the inlet plug and the outlet plug, the latter was again cut into two half cylinders (see Fig. 2). Polyoksymetylene (POM) spacers placed in the cut ensured open fractures of 1.2 mm aperture. Shrink tube held the core pieces and fracture spacers in place and an applied confinement pressure of 10 bar prevented bypass around the outside of the plug. The inlet core plug, denoted C, was separated from the outlet core halves by a transverse open fracture. The inlet plug was 28 mm long. The outlet core halves were 29 mm long and denoted A and B. The vertical fracture provided an escape flow path from the

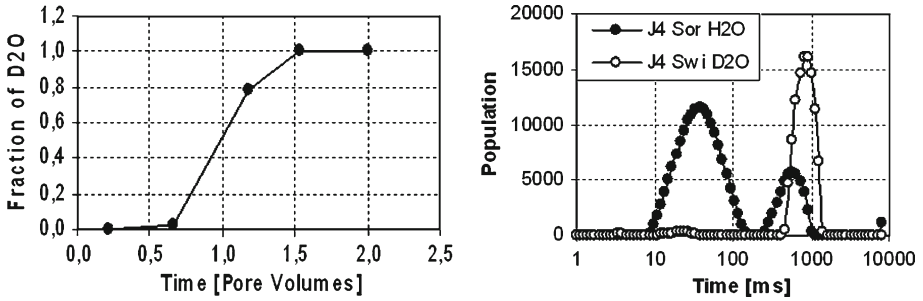

Fig. 4 (**a**) Fractional D2O-brine production during miscible displacement. (**b**) NMR spectroscopy indicating low residual regular brine saturation

transverse fracture to the system outlet. During the water floods, the core plug was positioned horizontally such that the open sagital fracture was aligned with gravity. The cutting process does not measurably alter the saturation or its distribution (Graue et al. 1999a, 2001a, b). During assembly, A and B were separated by 1.3 mm thick elongated POM-spacers. The absolute permeability of the sagital fracture was calculated to be 1.4×10^8 mD from the cubic law correlation between fracture aperture and permeability (Amyx et al. 1960) and later modified by Witherspoon et al. (1980),

$$k[\text{mD}] = 8.4 \cdot 10^9 \cdot A^2 \tag{1}$$

where A is the fracture aperture in cm. Assuming matrix permeability in the 1–10 mD range, the fracture-to-matrix permeability ratio is about 10^6–10^7.

Two-dimensional MRI was utilized in order to obtain high spatial resolution images of the fluid dynamics in the fractures. To distinguish between the two fluid phases, water and oil, the regular brine was displaced with D_2O brine at S_{or}. Results from the brine/brine displacement are shown in Fig. 4a and b. An efficient replacement was obtained (see Fig. 4a). As shown in Fig. 4b, the water NMR-signal at low relaxation time (20 ms) vanishes when water is displaced by D_2O (open dots), the NMR spectroscopy performed on the flooded core revealed a low remaining H_2O brine saturation of 1.3% PV.

Finally, the core was drained back to initial water saturation by a *n*-decane flood with an applied differential pressure of 2 bars/cm.

The MRI imaging sequence consisted of three image orientations:

1. Coronal (horizontal) slice through the center of the core (see Fig. 2b).
2. Three sagital (vertical) slices located within and on each side of the sagital fracture to determine the saturation in all the three matrix blocks and in the sagital fracture along the flow axis, see the small inserted images in Figs. 5 and 6.
3. A transverse (cross-sectional) slice showing the oil phase in the transverse fracture, shown as the large images in Figs. 5 and 6.

The dark circular band in the transverse images in Figs. 5 and 6 is the spacer separating the inlet core from the two core halves, with the slot at the top being an open, oil-filled section in the spacer. The dark rectangles in the sagital image are the two spacers which keep the vertical fracture open.

During the constant rate experiment, the differential pressure was continuously monitored. The core holder was made of composite material making it transparent to the RF and magnetic pulses used in MRI. The confining fluid was a non-imaging fluorocarbon, Fluorinert FC-40. Confinement pressure was kept constant at 10 bars.

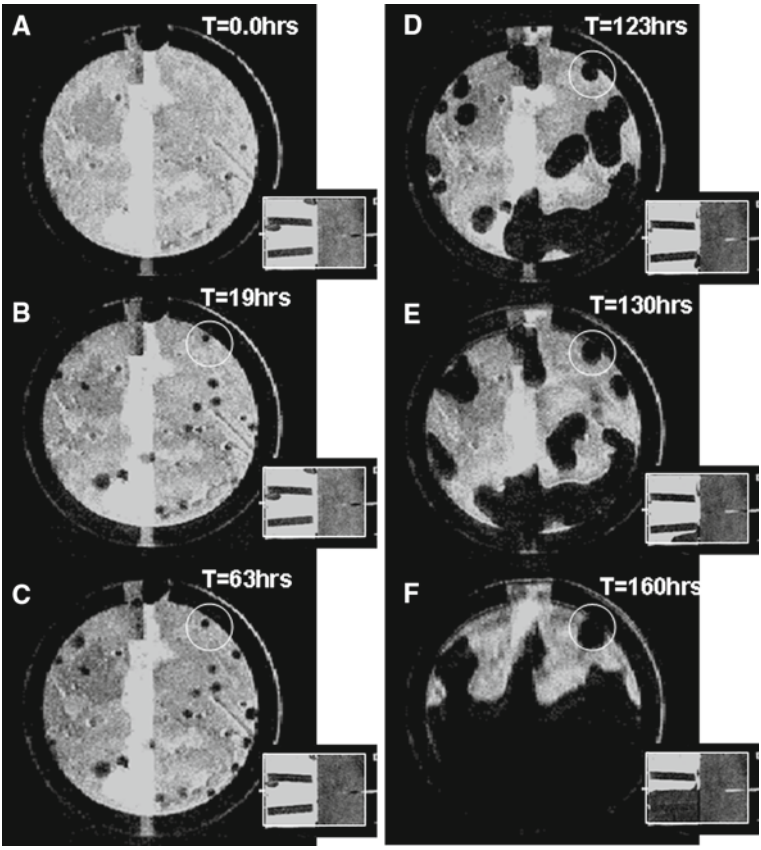

Fig. 5 Oil distribution in the transverse fracture (large image) and in the sagital fracture (small image) during the water flood at constant pressure. Water (D_2O) appears as the black phase

3 Results and Discussion

The main objective of this work was to investigate the possibility for the wetting phase to establish wetting phase bridges across the oil-filled, open fractures and thus exert a viscous pressure across the isolated, i.e., fracture-surrounded, core plug halves. The stacked core system was initially at S_{wi} with D_2O brine. D_2O does not respond to NMR signals and therefore shows up black in the MRI images. The fluid saturation dynamics is demonstrated by a series of images shown in Figs. 5 and 6. Each set of images corresponds to a time step; the large image showing the oil saturation distribution in the transverse open fracture and the associated smaller image showing the oil saturation in a vertical sagital slice through the center of the core system. The sagital image shows the oil saturation in the inlet core and in the open vertical fracture separating the two core halves at the outlet of the stacked core system. In the transverse image, the flow is from the inlet plug C, out of the image plane toward the reader to enter the outlet plug halves A and B. As only bulk oil is imaged, dark spots represents water bridges while dark grey spots represent a water droplet that has not established contact across the fracture. The black area surrounding the image is the spacer defining the open fracture.

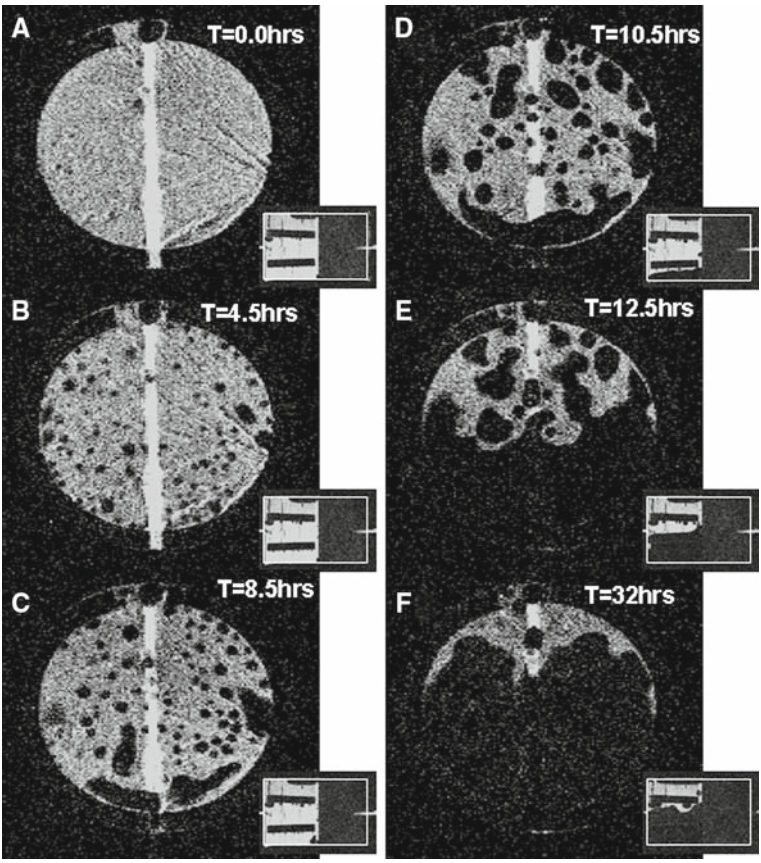

Fig. 6 Oil distribution in the transverse fracture (large image) and in the sagital fracture (small image) during the water flood at constant rate. Water (D_2O) appears as the black phase

In the small image, showing the sagital fracture, the injection of water is from the right through the un-fractured inlet block toward the open fracture on the left hand side of the image. The experiments were first conducted with a low constant differential pressure and then as a constant flow rate experiment at a much higher pressure.

3.1 Constant Pressure Waterflood

In the constant pressure experiment, a 14 cm high water column provided a differential pressure on the stacked cores of 14 mbar, corresponding to a viscous displacement pressure of 1 psi/foot. The level of the water column was never allowed to deviate more than 0.5 cm from its original level yielding an uncertainty of 4% in pressure. The first image, at 0.0 h, consists of the fracture filled with decane, a few air bubbles (small dark circles) trapped in the fracture and a portion of the matrix and fracture (the two grey halves and the light vertical streak, respectively). The latter two are observed because the MRI electronic slice-thickness is slightly greater than the fracture-thickness. The bright circular ring outside the spacer is decane-trapped between the spacer and the shrink tubing. After 19 h, Fig. 5b, water breakthrough from the inlet core is recorded as the formation of water (dark) bubbles. The

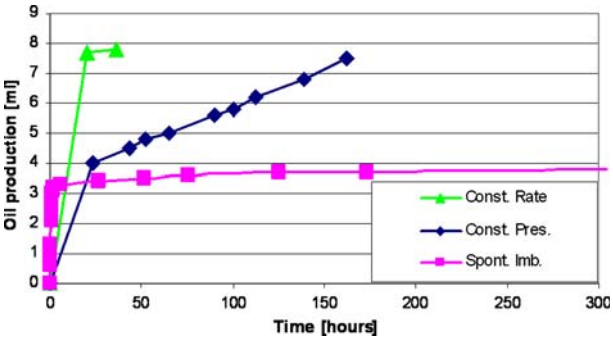

Fig. 7 Oil recoveries during the constant pressure and the constant flow rate experiments compared to oil recovery by spontaneous imbibition

corresponding sagital image shows that the vertical fracture is still primarily filled with decane. This implies that the water bridges stay on the fracture wall, with capillary forces preventing gravity segregation. Black circles indicate that the droplets touch the matrix on both sides of the fracture. A water bubble not spanning across the entire fracture aperture would appear on the images as a dark grey circle. To emphasize the stability of the water bridges, one single water bridge has been emphasized by highlighting it in a white circle through the entire water flood. Several other stable bridges can be found too.

By comparison, strongly water-wet experiments published by Graue et al. (2001b) and Aspenes et al. (2002a), show that the inlet plug reached its spontaneous imbibition endpoint of about 65% PV before water left the first block and entered the fracture. The flow mechanism in strongly water-wet chalk was dominated by film drainage along the exit surface of the first block to the bottom of the fracture, causing filling of the fracture at the rate of water injection. No water bridges were observed during the strongly water-wet experiments (Aspenes et al. 2002a).

The fact that the water appeared as separate droplets spread across the outlet surface of the inlet core plug indicated that the water front propagation in the first core was quite dispersed. This fits well with the sagital images and previous results (Aspenes et al. 2002a).

During the first 19 h, injection water propagated exclusively in the first core. Figure 5b confirms that no water has entered the fracture at this time. Image 5c was obtained at $t = 63$ h and shows that only three more water bridges developed in 44 h, the remaining bridges appear stable. However, at 63 h constant pressure production, the oil recovery is higher than accounted for by spontaneous imbibition alone. The water saturation in the fractures did not significantly change. Therefore, oil produced during this time period must come from the matrix. The oil production rate seems to be low and constant (Fig. 7), although spontaneous imbibition is believed to be ongoing in the isolated plug halves. The reason for this dramatic decline in the production rate is believed to be due to the limited access the isolated plug halves have on water through the 20–25 number of small water bridges. The bridges are measured to be approximately 1.5 mm in diameter which corresponds to the results from the low wettability case (Aspenes et al. 2002a). The fact that the water bridges during this period did not grow in size or in numbers is an indication of fairly stable water saturation at the outlet face of the inlet core.

At the next step shown in Fig. 5d, the water droplets start to grow and coalesce. Gravity now causes the droplets to fall to the bottom of the fracture. In the sagital image, this is observed by the entry of the dark water phase in the bottom of the sagital fracture. At this stage, the

oil recovery is almost twice the spontaneous imbibition potential. Further oil production is expected to be the hydraulic displacement from the open fractures. As the inlet and outlet lines are in the center of the core system, the sagital fracture is only half filled with water, i.e., the oil floats on top of the water.

The highlighted water bridge was stable from water breakthrough from the inlet core until the end of the experiment. This corresponded to 141 h or almost 6 days; exhibiting the stability of these water bridges.

From material balance and NMR analysis, the water saturation after the constant differential pressure flood is slightly above 50% PV and is approximately the same in all three pieces A, B, and C. By comparison, the spontaneous imbibition endpoint is 39% PV, hence the pressure gradient provided by the water bridges made a significant contribution to the oil recovery even in the isolated core plug halves.

3.2 Constant Flow Rate Waterflood

The same core system was oil-flooded back to initial water saturation of $S_w = 30\%$ using decane before being subjected to the constant rate injection experiment. The differential pressure applied on the system was an order of magnitude higher than in the constant pressure experiment, approximately 2psi. The objective was to see if the water bridges could sustain an even higher-pressure gradient across the isolated core halves.

The series of images in Fig. 6a–f show that the flow through the open fracture is similar to the constant pressure case. The main differences are the number of bridges and the time of their appearance. There are approximately 65 bridges in this case compared to 25 bridges on the constant pressure case. The sizes of the bridges are about the same size as in the constant pressure case; hence, the effective area of water flow has increased significantly. This happened because a higher water flux was forced to cross the fracture. It is interesting to see that the size of the bridges seems to be controlled by the wettability of the rock and not by the differential pressure applied across the open fracture. This corroborates a well-known theory, where the wettability at the exit face is assumed to control the droplet contact angle (Al-Maamari and Buckley 2000).

In addition to the fracture images, it was also decided to provide information on the matrix saturation development, see Fig. 8. This was done for several reasons. First, it provides data compatible for comparison with earlier fracture crossing experiments. Second, it will help keep track of the absolute saturation in the different core pieces, which provides information on the effect of the sagital fracture. Last but not the least, it brings more value to the fracture images because it shows the concurrent saturation in each matrix piece for every image. It shows that breakthrough of the first core happened when the saturation reached the spontaneous imbibition endpoint, where the capillary pressure was zero. It also shows that the water saturation of the two isolated plug halves started to increase immediately after the breakthrough from the inlet core. This was important in order to demonstrate water flux through the water bridges.

Interpreting the coalesce of the water bridges: Combining Figs. 6a and 8 and emphasizing the saturations in the open fractures and in the individual core plug matrices at 8.5 h, respectively, indicates two phenomena. One is that the water bridges coalesce because of an increase of water flux out of the first core. The reason for the increase in water flux may be, according to Fig. 6a, that the saturation in the inlet plug has reached a plateau; hence the core does not imbibe any more water. Water injected into the plug must, therefore be expelled into the fracture.

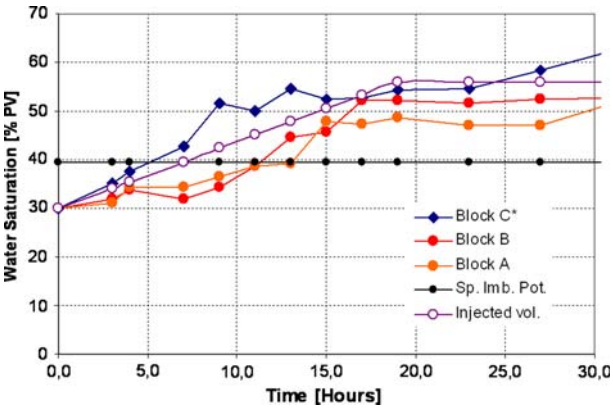

Fig. 8 Water saturation development in the inlet core plug and in the core halves during the constant flow rate waterflood

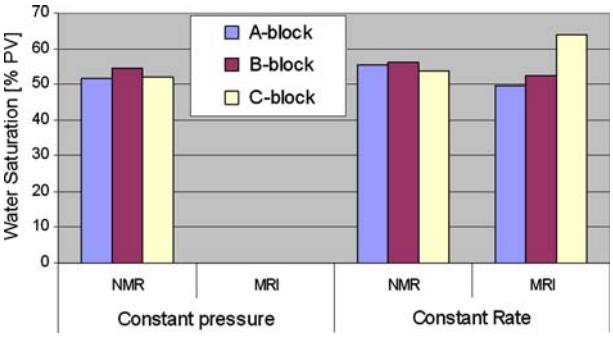

Fig. 9 NMR and MRI data comparison of water saturation of A, B and C-block at end of waterfloods

At the same time, when the water saturation in the inlet plug reached a plateau, the isolated core halves reached their spontaneous imbibition potential. This means that the role of the water bridges now changes from delivering water for spontaneous imbibition, to providing the differential pressure in the water bridges to the isolated core halves. Increased pressure in the water bridges will cause them to grow and finally coalesce with the surrounding bridges.

Finally, the dynamic MRI matrix saturation measurements indicate that the endpoint water saturation for the inlet plug is approximately 10% PV higher than in the isolated core halves. This maybe because the water bridges have a limitation in the pressure they can exert on the isolated core halves. Although the NMR measurement in Fig. 9 does not support the latter, both the MRI data and the material balance agree well. The NMR data is sensitive to the bulk volume of the core pieces, hence if a corner or edge of the fragile chalk material is damaged, this will affect the measurement.

The impact of increasing the waterflood differential pressure on the water saturation in the inlet and the isolated blocks are showed in Fig. 10 in blue and red curves, respectively. Spontaneous imbibition endpoint corresponds to zero differential pressure. The other pressure measurements presented in this article are measured during the water floods and therefore not comparable with static capillary pressure measurements. The motivation for plotting this graph, however, is to show the contribution to the oil recovery by applying increasing differential pressure across a matrix. At the constant injection pressure experiment applying

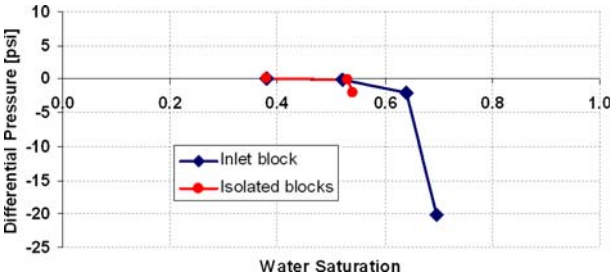

Fig. 10 Capillary imbibition curve for A and B-block in red, and C-block in blue

0.2psi, both the inlet block and the isolated blocks obtained water saturation of approximately $S_w = 53\%$ compared to the spontaneous imbibition endpoint of $S_w = 38\%$. In the constant rate experiment where 2psi were applied, the inlet block water saturation was increased to above $S_w = 60\%$, whereas the recovery from the isolated blocks remained about 53%. Therefore, increased differential pressure over the total system above 0.2psi will exceed the pressure that the water bridges are able to exert on the adjacent matrix blocks and hence no further oil will be recovered.

4 Conclusions

1. MRI imaging provided excellent dynamic information on the recovery mechanism in low permeable fractured chalk at nearly neutral wet conditions.
2. Despite the alternate escape path for the water phase, separate water bridges were shown to be stable for the entire duration of the 6-day experiment.
3. Water bridges transport water across open oil-filled fractures. This capillary contact provided a viscous component to the oil recovery in the outlet-isolated cores that exceeded the spontaneous imbibition potential by ca. 10% PV.
4. The effective cross-sectional area of water bridges was, due to the high water flux forced to cross the fracture, significantly higher in the constant rate experiment, however, the higher rate of injection and the higher number of bridges did not increase the recovery from the two isolated matrix blocks compared to the constant pressure experiment. The size of the bridges seemed to be controlled by the wettability of the rock and not by the differential pressure applied across the open fracture.
5. Further increased differential pressure (above 0.2psi) does not increase the recovery from the isolated blocks. The excess pressure exceeds the pressure that water bridges are able to exert on the adjacent matrix blocks and hence no further oil was recovered.

References

Agarwal, B., Hermansen, H., Sylte, J.E., Thomas, H.: Reservoir characterization of the Ekofisk field: A giant, fractured chalk reservoir in the Norwegian North Sea-History match. SPE 68096. Paper presented at the SPE reservoir simulation symposium, Huston, 14–17 February 1999

Al-Maamari, R.S.H., Buckley, J.S.: Asphaltene precipitation and alteration of wetting: can wettability change during oil production? In: SPE 59292. SPE/DOE Improved Oil Recovery Symposium, Tulsa, Oklahoma, April 3–5 (2000)

Amott, E.: Observations relating to the wettability of porous rock. Trans AIME **216**, 156–162 (1959)

Amyx, J.W., Bass, D.M., Whiting, R.L.: Petroleum Reservoir Engineering Physical Properties. McGraw-Hill Book Co., New York (1960)

Aspenes, E., Graue, A., Baldwin, B.A., Moradi, A., Stevens, J., Tobola, D.P.: Fluid flow in fractures visualized by MRI during waterfloods at various wettability conditions—emphasis on fracture width and flow rate. In: SPE 77338. Proceedings of the SPE Annual Technical Conference and Exhibition, San Antonio, Texas, 29 September–2 October (2002a)

Aspenes, E., Graue, A., Ramsdal, J.: In-situ wettability distribution and wetting stability in outcrop chalk aged in crude oil. In: Proceedings of the 7th International Symposium on Reservoir Wettability and Improved Oil Recovery, Tasmania, Australia, 12–15 March (2002b)

Bailey, N.A., Rowland, P.R., Robinson, D.P.: Nuclear measurements of fluid saturation in EOR flood experiments. In: Proceedings of 1981 European Symposium on Enhanced Oil Recovery, Bornmouth, England, 21–23 September (1981)

Firoozabadi, A., Hauge, J.: Capillary pressure in fractured porous media. SPE 18747 JPT **42**, 784–791 (1990)

Graue, A., Kolltveit, K., Lien, J.R., Skauge, A.: Imaging fluid saturation development in long coreflood displacements. SPEFE **5**(4), 406–412 (1990)

Graue, A.: Imaging the effect of capillary heterogeneites on local saturation development in long-core floods. SPEDC **9**(1), 57–64 (1994)

Graue, A., Viksund, B.G., Baldwin, B.A., Spinler, E.: Large scale imaging of impacts of wettability on oil recovery in fractured chalk. SPE J. **4**(1), 25–36 (1999a)

Graue, A., Viksund, B.G., Baldwin, B.A.: Reproducible wettability alteration of low-permeable outcrop chalk. SPE Res. Eng. Eval. April 134–140 (1999b)

Graue, A., Moe, R.W., Baldwin, B.A.: Comparison of numerical simulatons and laboratory waterfloods with in-situ saturation imaging of fractured blocks of reservoir rocks at different wettabilities. SPE59039. SPE International. Petr. Conference and Exh., Villahermosa, Mexico, 1–3 February, 2000a

Graue, A., Moe, R.W., Bognø, T.: Impacts of wettability on oil recovery in fractured carbonate reservoirs. In: Reviewed Proc.: International Symposium of the Society of Core Analysts, Abu Dhabi, United Arab Emirates, 18–22 October (2000b)

Graue, A., Aspenes, E., Moe, R.W., Baldwin, B.A., Moradi, A., Stevens, J., Tobola, D.P.: MRI tomography of saturation development in fractures during waterfloods at various wettability conditions. In: SPE 71506. Proc: SPEATCE, New Orleans, Louisiana, 30 September–3 October (2001a)

Graue, A., Bognø, T., Baldwin, B.A., Spinler, E.A.: Wettability effects on oil recovery mechanisms in fractured reservoirs. SPE74335, SPEREE **4**(6), 455–466 (2001b)

Graue, A., Aspenes, E., Bognø, T., Moe, R.W., Ramsdal, J.: Alteration of wettability and wettability heterogeneity. J. Petr. Sci. Eng. **33**, 3–17 (2002a)

Graue, A., Nesse, K.: Impact of fracture permeability on oil recovery in moderately water-wet fractured chalk reservoirs. SPE75165. In: Proc.: SPE/DOE Thirteenth Symposium on Improved Oil Recovery, Tulsa, Oklahoma, 13–17 April (2002b)

Graue, A., Baldwin, B.A., Aspenes, E.: Complementary imaging techniques applying NTI and MRI determined wettability effects on oil recovery mechanisms in fractured reservoirs. Paper presented at SCA annual conference, Pau, France, 2003

Hermansen, H., Thomas, L.K., Sylte, J.E., Aasboe, B.T.: Twenty five years of Ekofisk reservoir management. SPE 38927. Presented at SPE Annual Technical Conference and Exhibition, 5–8 October, San Antonio, Texas, 1998

Hermansen, H., Landa, G.H., Sylte, J.E., Thomas, L.K.: Experiences after 10 years of waterflooding the Ekofisk field, Norway. J. Petrol. Sci. Eng. **26**, 11–18 (2000)

Horie, T., Firoozabadi, A.: Laboratory Studies of capillary interaction in fracture/matrix systems. SPE August,353–360 (1990)

Labastie, A.: Capillary continuity between blocks of a fractured reservoir. In: 55th Annual Technical Conference and Exhibition, SPE, New Orleans, LA, 23–26 September (1990)

Lie, M.K.: Evaluation of outcrop chalk as analogues for north sea chalk reservoirs. Master Thesis in Reservoir Physics at University of Bergen (in Norwegian) (1995)

Lien, J.R., Graue, A., Kolltveit, K.: A Nuclear imaging technique for studying multiphase flow in a porous medium at oil reservoir conditions. Nucl. Instr. Meth. A, **271**, 693–700 (1988)

Saidi, A.M., Tehrani, D.H., Wit, K.: Mathematical simulation of fractured reservoir performance, based on physical model experiments. In: Proceedings of 10th World Petroleum Congress, paper PD10(3), Bucharest (1979)

Stones E.J., Mardsen, S.S., Zimmerman, S.A.: Gravity-induced drainage from fractured porous media. SPE 24042. Presented at the western regional meeting, Bakersfield, CA, 30 March–1 April, 1992

Sulak, R.M.: Ekofisk field: the first 20 years. SPE 20773, presented at the SPE annual technical conference and exhibition, New Orleans, 23–26 September, 1990

Thomas, L.K., Dixon, T.N., Evans, C.E., Vienot, M.E.: Ekofisk Water pilot. SPE 123120, presented at SPE annual technical conference and exhibition, Huston, Sept. 16–19, 1984. JPT February, pp. 221–232, 1987

Viksund, B.G., Graue, A., Baldwin, B., Spinler, E.: 2-D imaging of waterflooding a fractured block of outcrop chalk. In: Proc.: 5th Chalk Research Symposium, Reims, France, 7–9 October (1996)

Viksund, B.G., Eilertsen T., Graue, A., Baldwin, B., Spinler, E.: 2D-Imaging of the effects from fractures on oil recovery in larger blocks of chalk. In: Reviewed Proc.: International Symposium of the Society of Core Analysts, Calgary, Canada, 8–10 September (1997)

Witherspoon, P., Wang, J., Iwai, K., Gale, J.: Validity of cubic law for fluid flow in a deformable rock fracture. Water Resour. Res. **16**(6), 1016–1024 (1980)